Atmos. Chem. Phys. Discuss., https://doi.org/10.5194/acp-2019-164
Manuscript under review for journal Atmos. Chem. Phys.
Discussion started: 19 March 2019

Atmospheric Chemistry and Physics Discussions

Decadal Trends and Variability in Intermountain West Surface Ozone near Oil and Gas Extraction Fields

Ying Zhou[1], Huiting Mao[1], and Barkley C. Sive[2]

[1]Department of Chemistry, State University of New York College of Environmental Science and Forestry, Syracuse, NY, 13210, USA

[2]National Park Service, Air Resources Division, Lakewood, CO 80225, USA

Corresponding author: H. Mao (hmao@esf.edu)

Atmos. Chem. Phys. Discuss., https://doi.org/10.5194/acp-2019-164
Manuscript under review for journal Atmos. Chem. Phys.
Discussion started: 19 March 2019

Atmospheric Chemistry and Physics Discussions

Abstract

Decadal trends in the annual fourth-highest daily maximum 8-hour average (A4DM8HA) ozone (O_3) were studied over 2005 – 2015 for 13 rural/remote sites in the U.S. Intermountain West. No trends were observed in A4DM8HA O_3 at two reference sites, which are located upwind of and thus minimally influenced by emissions from oil and natural gas (O&NG) basins. Trends, or a lack thereof, varied widely at other 11 sites in/near O&NG basins resulting from different controlling factors rather than a simplistic, uniform one. The decreasing trends at Mesa Verde (-0.76 ppbv/yr) and Canyonlands National Park (-0.54 ppbv/yr) were attributed to a 37% decrease in natural gas production in the San Juan Basin and 35% emission reductions in coal-fired electricity generation, respectively. The decreasing trend (-1.21 ppbv/yr) at Wind Cave National Park resulted from reduced solar radiation due to increasingly frequent precipitation weather. The lack of trends at remaining sites was likely caused by the increasing O&NG emissions and decreasing emissions from other activities. Wintertime O_3 stagnant events were associated with the Arctic Oscillation (AO). Box model simulations suggested that both volatile organic compounds (VOCs) and nitrogen oxides emission reductions during negative AO years while VOC emission reductions alone in positive AO years could effectively mitigate high wintertime O_3 within the O&NG basins. Our findings suggest that emissions from O&NG extraction likely played a significant role in shaping long-term trends in surface O_3 near/within O&NG basins and hence warrant consideration in the design of efficient O_3 mitigation strategies for the Intermountain West.

Atmos. Chem. Phys. Discuss., https://doi.org/10.5194/acp-2019-164
Manuscript under review for journal Atmos. Chem. Phys.
Discussion started: 19 March 2019

Atmospheric Chemistry and Physics Discussions

1 Introduction

Tropospheric ozone (O_3) is a short-lived trace gas that either originates naturally from the stratosphere (Stohl et al., 2003) or is produced in situ by photochemical oxidation of nitrogen oxides (NO_x) and volatile organic compounds (VOCs) or carbon monoxide (CO) (e.g., Monks et al., 2009). On 1 October 2015, the U.S. Environmental Protection Agency (EPA) lowered the National Ambient Air Quality Standard (NAAQS), namely the O_3 design value, to 70 ppbv to improve protection of public health and welfare (EPA, 2015). Unlike in the eastern U.S., where NO_x emission reductions have led to O_3 declines, in the Intermountain West no decreasing trends were observed over 1988 – 2014 and surface O_3 could exceed the NAAQS in both winter and summer (Schnell et al., 2009; Cooper et al., 2012; Edwards et al., 2014; Lin et al., 2017). Most studies attributed the increasing background O_3 trends over the western U.S. to increasing anthropogenic Asian emissions (e.g., Cooper et al., 2012; Parrish et al., 2012; Lin et al., 2017). Lefohn et al. (2012) found that stratospheric intrusion affected the interannual variability of surface O_3 at both high- and low-elevation sites. However, a multi-model study suggested that surface O_3 in the U.S. was far more sensitive to domestic emission changes than to global emission changes in spring and summer (Reidmiller et al., 2009). Thus, long range transport from Asia and stratospheric intrusion may not be the sole contributors to the observed increasing trends in western U.S.

Recent expanded use of horizontal drilling and hydraulic fracturing technologies enabled access to more natural gas resources in shale deposits (EIA, 2015). Extraction of oil and natural gas (O&NG) can result in the emission of O_3 precursor gases and episodes of elevated O_3 mixing ratios in O&NG production basins frequently exceeding the NAAQS. Most notable were the episodes that occurred during the cold season in the Intermountain West (Carter and Seinfeld,

2012; Edwards et al., 2014; Rappenglück et al., 2014; Schnell et al., 2009). Carter and Seinfeld (2012) studied four O_3 episodes in the Upper Green River Basin in Wyoming and found one episode highly NO_x-sensitive and the others VOCs-sensitive. Edwards et al. (2014) used a box model to simulate a stagnant 6-day high O_3 event in the Uintah Basin and found that carbonyl photolysis was the dominant oxidant source. McDuffie et al. (2017) studied O_3 in the Colorado Northern Front Range (NFR) in summer 2012 and found that O&NG emissions contributed to 17% of the modeled maximum photochemically produced O_3. To the best of our knowledge, no studies have investigated the long-term impact of expanded O&NG extraction activities on O_3 over the intermountain U.S. using more than ten years of measurement data.

The effect of emissions from O&NG production on surface O_3 is difficult to quantify because a wide range of factors work together to determine the mixing ratio of O_3 at a given location, such as other anthropogenic emissions, natural emissions, transport processes, stratospheric intrusion, O_3 photochemistry, and changing global climate (Parrish et al., 2013); however, the significance of these factors varies by season. For example, the number of high O_3 days in summer was strongly correlated with wildfire burned area over the western U.S. as wildfires are important sources of NO_x, CO, and VOCs (Jaffe et al., 2008; Jaffe and Wigder, 2012). The frequency and intensity of wildfires in the western U.S. may be increasing, driven by increasing temperatures, earlier snowmelt, drier conditions, and accumulation of fuels (Westerling et al., 2006; Jaffe et al., 2008). Moreover, all components that can impact the distribution of O_3 are associated with varying atmospheric circulation patterns on interannual to decadal time scales (e.g., Lin et al., 2014; Zhou et al., 2017). For instance, more frequent stratospheric intrusion events occurred in late spring, when the polar jet meandered towards the western U.S. following La Nina events (Lin et al., 2014). Therefore, it is fundamentally

96 important, yet also challenging, to extract the impact of increasing emissions from O&NG
97 production on surface O_3 levels from all of these various factors. However, these findings could
98 ultimately lead to improved modeling and to better assess the efficacy of emission controls.
99 A most common approach to assess the influence of a certain factor or source on O_3
100 concentrations is through model simulations (e.g., Rodriguez et al., 2009; Lin et al., 2017).
101 However, the application of current chemical transport models used to investigate the impact of
102 emissions from O&NG extraction on tropospheric O_3 is particularly challenging because of the
103 large uncertainties existing in the emission inventories of O&NG extraction (Pétron et al., 2014;
104 Helmig et al., 2014; Ahmadov et al., 2014; Thompson et al., 2017; Allen, 2014; Allen, 2016).
105 Past studies have found that the emissions of methane and VOCs from oil and gas extraction was
106 largely underestimated (Karion et al., 2013; Ahmadov et al., 2014). Therefore, for this study the
107 approach of data analysis was chosen in order to provide measurement-based contribution
108 estimates of various factors.
109 Specifically we investigated the decadal impact of emissions from O&NG extraction on
110 variability and long term trends of surface O_3 in the Intermountain West since 2005, when
111 O&NG extraction activities started to expand rapidly (EIA, 2015). In this study, we used long
112 term O_3 measurement data obtained from the National Park Service (NPS), Clean Air Status and
113 Trends Network (CASTNET), and Wyoming Department of Environmental Quality (WDEQ),
114 many of which are from Class I areas as designated by the Clear Air Act. However, some of
115 these sites have been reportedly influenced by O&NG emissions since 2005 (EIA, 2015). This
116 study was focused on the summer and winter, when exceedances of NAAQS tended to occur in
117 the Intermountain West (Edwards et al., 2014; Lin et al., 2017).

118 **2 Materials and Methods**

Atmos. Chem. Phys. Discuss., https://doi.org/10.5194/acp-2019-164
Manuscript under review for journal Atmos. Chem. Phys.
Discussion started: 19 March 2019

119 **2.1 Site Selection and Data description**

120 Long term surface O_3 observations were available at 18 sites in remote and rural areas of
121 the U.S. Intermountain West (Figure 1 and Table S1). Among the 18 sites, 11 sites are located
122 within 100 km of a shale play and are more likely affected by emissions from O&NG extraction
123 activities (Figure 1). Specifically, Mesa Verde National Park (MEVE), Pinedale, WY (PNDE),
124 Centennial, WY (CNTL), Gothic, CO (GTHC), Rocky Mountain National Park (ROMO), and
125 Wind Cave National Park (WICA) are located near O&NG Basins, while Canyonlands National
126 Park (CANY), Dinosaur National Monument (DINO), Rangely, CO (RANG), Meeker, CO
127 (MEEK), and Campbell, WY (CAMP) are located within O&NG basins. Of the remaining 7 sites,
128 Yellowstone National Park (YELL) and Craters of the Moon National Monument and Preserve
129 (CRMO) were the only two sites located upwind O&NG fields and were therefore used as
130 reference sites to investigate the decadal O_3 change with minimal influence of O&NG emissions.
131 Four sites, Great Basin National Park (GRBA), Zion National Park (ZION), Grand Canyon
132 National Park (GRCA), and Petrified Forest National Park (PEFO), were found, based on
133 backward trajectory cluster analysis, to often receive air masses influenced by nearby
134 anthropogenic emissions from Las Vegas (Section S2). Badlands National Park (BADL), located
135 more than 100 km away from the shale play, was impacted one third of the time by air masses
136 from O&NG activity in the Powder River Basin during the 2005 – 2015 decade (Section S2).
137 Therefore, GRBA, ZION, GRCA, PEFO and BADL were not included in the analysis of this
138 study.

139 Continuous hourly measurements of O_3 were available at each site. We calculated the
140 annual fourth-highest daily maximum 8-hour average (A4DM8HA), upon which the O_3 design
141 value was based, for the 13 monitoring sites and their trends were examined through ordinary

142 linear least-square regression. The trends were also calculated separately for 5th, 50th, 95th
143 percentiles of daily maximum 8-hour average (DM8HA) O_3 in winter and summer.

144 **2.2 Box Model**

145 Box model simulations were performed using BOXMOX (Knote et al., 2015) and the
146 NCAR Tropospheric Ultraviolet and Visible Radiation Model (TUVv5.3.1) (Madronich et al.,
147 1998). BOXMOX is an extension to the Kinetic PreProcessor which allows an easy set up for
148 zero dimension box model simulations (Knote et al., 2015). We selected the Master Chemical
149 Mechanism (MCM v3.3) for the model chemistry scheme. The MCM is a near-explicit chemical
150 mechanism including gas-phase tropospheric degradations of 74 VOCs and OVOCs with a total
151 of 5259 species of and 15176 reactions (Jenkin et al., 2015).

152 All simulations were initialized with observations from field campaigns in the
153 Intermountain West. These campaigns were Uintah Basin Winter Ozone Study (UBWOS) over
154 2012 – 2014 (Edwards et al., 2013), Nitrogen, Aerosol Composition, and Halogens on a Tall
155 Tower (NACHTT) in 2011 (Swarthout et al., 2013), and Front Range Air Pollution and
156 Photochemistry Éxperiment (FRAPPÉ) in 2014 (Pfister et al., 2017). Section S8 provides
157 detailed information about field campaign measurements. The modeled mixing ratios of CO,
158 CH_4, NO, NO_2, and non-methane VOCs were forced to match the measured diurnal profiles by
159 introducing turbulent mixing to the model (Knote et al., 2015; Section S8.3). Therefore, the "box"
160 can dynamically exchange with its surroundings. The model was integrated forward with a time
161 step of 10 minutes until the concentrations reach a diurnal steady state, when the cycles of
162 simulated species exhibit less than 0.01% variation from the previous day (Edwards et al., 2013).
163 The last 24 h were used to represent the simulated diel cycles. Section S8 provides further
164 information on the model treatment of all chemical observations.

Atmos. Chem. Phys. Discuss., https://doi.org/10.5194/acp-2019-164
Manuscript under review for journal Atmos. Chem. Phys.
Discussion started: 19 March 2019

Atmospheric Chemistry and Physics Discussions

3. General Characteristics in Long-term Variations of O_3

First, changes in the A4DM8HA were examined for the 13 sites before and after 2005, when O&NG extraction started expanding rapidly. Before 2005, statistically significant increasing trends were observed at the reference site CRMO as well as three other sites, CANY, CNTL, and PNDE, near O&NG basins with no significant trends at the other sites (Figure 2). After 2005, no significant trends were found at the two reference sites (CRMO and YELL, Table S2). Among the 11 sites near/within the O&NG basins, significant decreasing trends were observed at CANY (-0.54 ppbv yr^{-1}), MEVE (-0.76 ppbv yr^{-1}), and WICA (-1.21 ppbv yr^{-1}), with no significant trends at the other sites (Table S2). The decadal (2005 – 2015) mean of the A4DM8HA reached or exceeded 70 ppbv, the current NAAQS, at three sites, DINO (82.7 ppbv), RANG (72.7 ppbv), and ROMO (75.1 ppbv).

Trends in seasonal 5^{th}, 50^{th}, 95^{th} percentiles of DM8HA O_3 were further examined (Table S3). At the two reference sites, no trend was observed in any seasonal percentiles of DM8HA O_3 at YELL, while statistically significant decreasing trends (-0.14 to -1.18 ppbv yr^{-1}) were observed in wintertime $50^{th}/95^{th}$ and summertime $5^{th}/50^{th}/95^{th}$ percentile values at CRMO. Significant decreasing trends were also observed at 4 sites located in/near O&NG basins. Specifically, at MEVE significant decreasing trends of -0.49 to -0.63 ppbv yr^{-1} were found in seasonal $50^{th}/95^{th}$ percentile values in both winter and summer (Table S3). In contrast, significant decreasing trends were only found in summertime $5^{th}/50^{th}$ at CANY, summertime 95^{th} at WICA, and wintertime $50^{th}/95^{th}$ percentile values at GTHC. Overall seasonal median values near the O&NG extraction basins showed relatively more consistent patterns of interannual variation at relatively low elevation sites (i.e., CANY, DINO, MEEK, RANG, CAMP, MEVE, and WICA) in winter, while in summer, large differences were found between sites (Figure 3).

Previous studies have examined long term trends in tropospheric O_3 for varying time periods over the continental U.S. (e.g., Cooper et al., 2012; Cooper et al., 2014; Lin et al., 2017; Gaudel et al., 2018). Gaudel et al. (2018) assessed surface O_3 trends at 2702 non-urban sites from the Tropospheric Ozone Assessment Report (TOAR) database. They found significant increasing trends (0.5 to 1.0 ppbv yr^{-1}) in daytime average O_3 at 6 sites in the Intermountain West and no trends at 8 other sites including MEVE, PNDE, YELL in winters of 2000 – 2014 (Gaudel et al. 2018). However, in this study a significant decreasing trend (-0.49 ppbv yr^{-1}) in wintertime 95th percentile values was observed at MEVE after 2005, possible causes for which are discussed further in Section 4. In summers of 2000 – 2014, significant decreasing trends (~ -0.5 ppbv yr^{-1}) in daytime average O_3 were observed by Gaudel et al. (2018) at most sites including CRMO, PNDE, CANY, MEVE, which was consistent with trends we observed (Table S3).

The following questions arose from examining the above characteristics in surface O_3 at the 11 sites near/in O&NG basins:

1) Were the decreasing trends in A4DM8HA at MEVE, CANY, and WICA potentially linked in some ways to changes in O&NG production activities nearby?
2) Was there seasonal variation in the influence of emissions from O&NG extraction on seasonal DM8HA O_3?
3) Were there changes of O_3 production regime as a result of emissions from O&NG basins over the years?

These questions are addressed in the following sections with the goal to delineate the role of emissions from O&NG production in long-term trends in surface O_3 at the 11 sites.

4. Contribution of emissions from O&NG production vs other anthropogenic sources

The two reference sites, YELL and CRMO, are located >100 km upwind of O&NG

basins (Figure 1) and exhibited no trends in A4DM8HA after 2005. In comparison, decadal trends of O_3 at the 11 sites situated in or near the O&NG extraction basins ranged widely, indicating complex influence of varying changes in emissions from O&NG production activities combined with other anthropogenic sources.

The strong decreasing trends in A4DM8HA at MEVE and CANY appeared to be driven by significant reductions of emissions from local industry during 2005 – 2015. MEVE is located near the San Juan Basin (Figure 1), the second largest natural gas field in the U.S. A 37% decrease in natural gas production was reported in the San Juan Basin over 2005 – 2015 (Figure 4a), subsequently leading to reduced emissions of O_3 precursors. Meanwhile NO_x emissions from other sectors in San Juan County decreased by 65% from 80,734 tons in 2005 to 27,996 tons in 2014 (Table S4). This is supported by the strong declines in tropospheric NO_2 column densities in summer at a rate of ~ -2.8×10^{13} molecular cm^{-2} yr^{-1} ($p \leq 0.05$) surrounding MEVE around the San Juan Basin over 2005 – 2015 (Figure 4b). Decadal changes were not computed for winter due to scarce wintertime column NO_2 retrievals over the Intermountain West. Because O_3 production in U.S. rural areas was typically sensitive to changes in NO_x emissions (Cooper et al., 2012), the decreasing NO_x emissions associated with reduced natural gas production and emission controls in other sectors were most likely the primary cause for the significant decrease in the A4DM8HA at MEVE (-0.76 ppbv yr^{-1}) during 2005 – 2015. The significant decreasing trend in the A4DM8HA observed at CANY was possibly a result of the declining extraction of coalbed methane (CBM) in the Paradox Basin and emission reductions in coal-fired electricity generation in Emery County. Historically, Emery County in the Paradox Basin was the main CBM producer. Permitting activities for CBM extraction have declined by 48% over 2005 – 2015 resulting from lower natural gas prices (NGI, 2018) (Figure 4a). Meanwhile, NO_x

emissions from coal-fired electricity generation, contributing ~88% of the total NO_x emissions in Emery County, decreased by 35% from 28,407 tons in 2005 to 18,336 tons in 2014 (Table S4). As a result of these changes, significant decreasing trends in the seasonal 95th percentile would be anticipated, but were not observed in both winter and summer. This indicates that there are additional factors producing significant influences on O_3 in the area, which are further investigated in Sections 5 – 6.

No trend was observed in the A4DM8HA O_3 at CAMP, which was likely associated with changes in natural gas vs. oil production activities in the Powder River Basin. CAMP is located within the Powder River Basin, which is traditionally known for its coal production and has been one of the fastest growing oil producing regions in recent years. While natural gas production in Campbell County decreased by 62% (Figure 4a), oil production in Campbell County increased from 9×10^8 barrels in 2005 to 2.3×10^9 barrels in 2015 (http://wogcc.wyo.gov/). WICA is located downwind of the Powder River Basin, experiencing a significant decreasing trend in the A4DM8HA at a rate of 1.21 ppbv yr^{-1} (p = 0.05) over 2005 – 2014. Curiously, total NO_x emission increased by 29% from 1,327 tons in 2005 to 1,712 tons in 2014 in Custer County, where WICA is located (Table S4). The decreasing A4DM8HA at WICA is attributed to other factors, as discussed in Section 6.

DINO, RANG, and MEEK are located within the Uintah-Piceance Basin O&NG fields (Figure 1). Increased emissions, most likely from a 68% rise in natural gas production over 2005 – 2015 in the Uintah Basin (Figure 4a), together with snow cover (Edwards et al. 2014; Section xx), could have contributed to very high A4DM8HA O_3 at DINO and RANG. Meanwhile, NO_x emissions from highway vehicles decreased by 86% in Uintah County (Table S4). MEEK, in Rio Blanco County, is located at the eastern edge of the Piceance Basin and relative lower 4DM8HA

257 O_3 (64.1 ppbv) was observed, and trends were not examined for the site's short data record (6
258 yrs).

259 The four high-elevation sites, ROMO, PNDE, CNTL, and GTHC, experienced no trends
260 in their A4DM8HA due likely to opposite changes in emissions from O&NG production, urban
261 sources, and stratospheric intrusion (or a lack thereof). ROMO is located to the west of the
262 Denver-Julesburg Basin and has experienced northwesterly and southeasterly wind most
263 frequently over 2005 – 2015 (Figure 5a) with higher O_3 (>60 ppbv) from the east and southeast
264 (Figure 5e). Natural gas production in Weld County increased by nearly a factor of 3 from 2009
265 to 2015, which coincided with use of horizontal drilling starting in 2009 (Figure 4a). Meanwhile
266 the NO_x emission reductions of ~37% from the urban area of Denver offset the effect of
267 increased NO_x emissions from O&NG extraction, as evidenced by the significant declines in
268 tropospheric column NO_2 (Figure 4b).

269 PNDE is located to the north of the Green River Basin, which has two U.S. largest
270 natural gas fields, i.e., Pinedale Anticline and Jonah Field. Natural gas production increased
271 steadily over 2005 – 2010 followed by a decline in 2011 and onward. At PNDE, while the
272 dominant winds were from the northwest, southeast, and northeast (Figure 5b), O_3 mixing ratios
273 corresponding to southwesterly wind, from where expansive O&NG extraction occurred, reached
274 higher than 60 ppbv (Figure 5f). Overall, no trend was observed in natural gas production in
275 Sublette County in the basin (Figure 4a), which was consistent with the relative constant
276 A4DM8HA at PNDE.

277 CNTL was located to the north of the North Park Basin and southeast of the Green River
278 Basin (Figures 1 and 5g). In the past decade, natural gas production in Jackson County in the
279 North Park Basin decreased by 72% (Figure 4a) and oil production increased comparatively by

73%, which likely contributed to constant A4DM8HA O_3 at CNTL. Similar to all high-elevation sites (i.e., ROMO, PNDE, CNTL), GTHC is another site located at the mountain ridge. The high O_3 concentrations from the north (> 65 ppbv) and southwest (> 52 ppbv) indicate that the site was likely under the influence of aforementioned opposite changes in emissions from the North Park Basin, Denver-Julesburg Basin, and San Juan Basin (Figures 5d and h) ultimately resulting in the site exhibiting no trend in the A4DM8HA.

5. Contributions of transport from the Arctic and the West Coast and stratospheric intrusion in winter

Winter seasonal median DM8HA O_3 showed consistent interannual variation with higher O_3 levels (38 – 59 ppbv) in 2011 and 2013 whereas lower values (32 – 44 ppbv) in 2012 at the two references sites and most sites near/within O&NG basins, except the three high-elevation sites (i.e., GTHC, ROMO, CNTL) (Figures 3c-d). Seasonal 5^{th} and 95^{th} percentile values exhibited similar patterns (not shown). Site average O_3 mixing ratios exceeded the decadal average 41 ppbv in 2006, 2008, 2010, 2011, 2013, and were below average in 2007, 2009, 2012, 2014, 2015. The difference of the 850 hPa geopotential height between the higher and lower O_3 years is shown in Figure 6a. A pronounced positive difference of ~60 geopotential meters (gpm) was observed over the Arctic polar region and a negative difference of ~ 40 gpm over the midlatitudes. This pattern strongly indicates a negative (positive) phase of Arctic Oscillation (AO) associated with a higher (lower) O_3 winter in the Intermountain West. Indeed significant negative correlations (-0.91 to -0.58) were found between the AO index and winter seasonal $50^{th}/95^{th}$ percentile DM8HA O_3 at most sites, including the reference site YELL over 2005 – 2015 (Table 1 and Figure 6b). Significant correlation was not found at the other reference site CRMO, which is located to the south of the Pioneer Mountains and received few air masses (3%)

303 from the north (Figure S1b). Weaker correlations were also observed in the seasonal median
304 DM8HA at CNTL and PNDE. During a longer time period dating back to years prior to 2005,
305 significant negative correlation was observed between seasonal median DM8HA O_3 and the AO
306 index at the reference site YELL (-0.45 over 1997 – 2005), as well as at CANY (-0.47 over 1993
307 – 2015), CNTL (-0.46 over 1990 – 2015), and ROMO (-0.67 over 1988 – 2015). This indicates
308 that the impact of AO on wintertime surface O_3 has been consistently significant during different
309 time periods over the past decades in the Intermountain West.

310 The negative correlation between AO and wintertime O_3 could be a result of multiple
311 factors, including transport from the Arctic and California, in situ O_3 photochemical production,
312 and stratospheric intrusion. While long-term O_3 trends in lower percentiles could be influenced
313 by long-range transport, O_3 in higher percentiles was more sensitive to local emissions and
314 extreme events (Lin et al., 2017). First, the influence of transport from the Arctic was examined.
315 Artic influence would be foremost demonstrated in surface temperature. During negative AO
316 years, frigid winter air masses could extend far into the middle of North America, contributing to
317 relatively cold temperatures over the U.S. Intermountain West (Hess and Lamarque, 2007).
318 Significant positive correlation was found between the AO index and surface temperature at
319 CANY, DINO, MEEK, RANG, and GTHC. Except for GTHC, all sites are located within the
320 basins and weaker positive correlations were observed at other sites, except for CNTL, the
321 highest elevation site in this study (3175 m amsl) (Table 1 and S1). Significant negative
322 correlation was also found between surface temperature and wintertime O_3 at sites within the
323 basin (i.e., CANY, DINO, MEEK, and RANG), with the potential effect of stratospheric
324 intrusion removed (Partial correlation in Table 1). Higher correlation coefficients were found in
325 seasonal 50^{th}/95^{th} DM8HA at DINO, MEEK, and RANG, indicating that the sites were more

likely under local influence (Table 1). During a colder winter with constant snow cover, high concentrations of O_3 precursors emitted from O&NG extraction were trapped in a shallow boundary layer within the basins followed by strong O_3 photochemical production during daytime leading to the highest O_3 mixing ratios of the season (Schnell et al., 2009; Edwards et al., 2014). For sites outside the basins that are exposed to distant sources (Figure S1), the significant correlation between wintertime median DM8HA O_3 and the AO index is a strong indication of impacts of long-range transport from source regions afar.

Backward trajectory simulations suggest that long distance transport from the West Coast may obscure the correlation between the AO index and surface O_3 at MEVE, ROMO, YELL, WICA, CNTL, and PNDE. A total of 902 five-day backward trajectories were performed at each site during winters of 2006 – 2015 (Figure 7). The difference in numbers of trajectories between high and low O_3 years suggests that more air masses reached the six sites coming from low altitudes (<900 hPa) over the area of southern California and Arizona, centered around 32.5 °N/120 °W during high O_3 years (Figure 7). At YELL, WICA, PNDE, ROMO, and CNTL, more than 80 backward trajectories passed through the surface of California (Figure 7), where large amounts of O_3 could be produced from emissions of facilities in urban areas (Ryerson et al., 2013). Huang et al. (2013) also found that anthropogenic emissions from southern California could contribute 1 – 15 ppbv to surface O_3 in air masses transported to the Intermountain West. Additionally, more than 20 trajectories originating at YELL, CNTL, ROMO, and MEVE came from higher altitudes (>700 hPa) in the north (>45 °N) during high O_3 years (Figure 7). During negative AO (high O_3) years, cold Arctic mid-tropospheric air rich in O_3 would cross Canada and reach the U.S. Intermountain West more frequently (Hess and Lamarque, 2007). This is in part evidenced in the significant negative correlation (r = -0.49, p = 0.01) between the AO index and

lower tropospheric O_3 at Edmonton, Alberta, Canada over 1988 – 2014 (Figure S2), indicating stronger impacts of Arctic mid-tropospheric O_3 on the Intermountain West during negative AO years.

Stratospheric influence on surface O_3 was also examined. One of the physical characteristics of stratospheric air is high values of potential vorticity (PV). The differences in PV between high and low O_3 years exhibited positive anomalies of ~0.5 PV (10^{-6} $m^2s^{-1}kg^{-1}K$) in the mid-troposphere (315 K) over the Intermountain West (Figure 8). Significant negative correlations of -0.64 ($p < 0.01$) over 1988 – 2015 and -0.76 ($p = 0.01$) over 2005 – 2015 were found between PV and the AO index over the study region (37.5 °N – 45 °N, -102.5 °W – -110°W). This indicated that stratospheric intrusion over the Intermountain West was associated with the negative AO with a strong impact at sites outside the basins over the region.

6. Effects of precipitation weather on summertime O_3

We found that summertime O_3 in the Intermountain West was strongly correlated with relative humidity and the wildfire index total fire index (TFI) (Table S6). Studies have suggested that in the Intermountain West, summertime O_3, especially the seasonal high percentile levels, was impacted by photochemical production from wildfire emissions (Table S6; Jaffe and Wigder, 2012; Lu et al., 2016). To avoid repeating the extensive body of literature on this topic, our own analysis of the effect of wildfires on O_3 can be found in Section S7. One key point coming out of our analysis was, with fire influence removed as indicated in partial correlation, significant negative correlations between summertime O_3 and relative humidity were found at the two reference sites (CRMO and YELL), as well as at the 7 O&NG emission influenced sites (CANY CAMP, MEEK, RANG, ROMO, PNDE, and WICA) (Table S6). Further investigation, detailed

371 as follows, revealed that this correlation essentially illuminated the effect of reduced solar
372 radiation on O_3 production caused by cloudiness associated with precipitation weather.

373 In the Intermountain West, precipitation varies by elevation and latitude among other
374 factors (Williams et al., 1962). The decadal summertime average precipitation abundance was
375 0.17 kg m^{-2} for the reference site YELL and 0.15 – 0.27 kg m^{-2} for GTHC, CNTL, ROMO, and
376 WICA, which were higher than that at CRMO (0.08 kg m^{-2}) and the remaining sites (Figure 9a).
377 YELL, GTHC, CNTL, ROMO, and WICA are located in the mountains, where localized
378 convective storms could develop quickly in summer leading to higher precipitation amounts
379 (Williams et al., 1962) and naturally, more cloudiness at these five sites compared to the other
380 sites located within the basins. This is consistent with the significant negative correlations
381 between summertime O_3 and relative humidity at CNTL, ROMO, WICA, and the reference site
382 YELL (Table S6). Note that no significant partial correlation was found between summertime O_3
383 and relative humidity at GTHC, indicating that summertime O_3 at this site was mostly influenced
384 by wildfire emissions. Significant correlations were also found between solar radiation and
385 summertime median DM8HA O_3 at CNTL (r = 0.67, p = 0.05), ROMO (r = 0.43, p = 0.09),
386 WICA (r = 0.62, p = 0.05), and YELL (r = 0.72, p = 0.01). These results indicate that reduced
387 solar radiation flux near the surface resulting from increased cloudiness accompanying increased
388 precipitation resulted in less O_3 production over the mountain ranges.

389 Situated on the southern section of the Black Hills, WICA received the highest
390 summertime average precipitation of 0.27 kg m^{-2} (Figure 9a). Total Precipitation showed a
391 significant negative correlation with summertime median DM8HA O_3 at WICA (r = -0.65, p =
392 0.04, Figure 9b). As noted in Section S7, the decadal highest summertime median DM8HA O_3
393 was observed in 2012 at 7 sites because of the decadal maximum wild fire emissions. WICA was

394 the exception with its 2012 summertime median DM8HA O_3 being the second largest (58 ppbv)
395 of the decade, compared to the largest value of 61 ppbv in 2006 (Figure 3b), despite the fact that
396 the decadal maximum TFI occurred in 2012 (0.022 g NO_x m^{-3} in Figure 9b). O_3 levels were
397 expected to be lower in the summer of 2006 because it had the least influence of wildfire
398 emissions evidenced by a very low TFI value (0.010 g NO_x m^{-3}) (Figure 9b). However, the
399 decadal minimum precipitation (0.18 kg m^{-2}) in the summer of 2006 counteracted the effect of
400 less wildfire emissions (Figure 9b). By comparison, increased cloudiness accompanied more
401 precipitation (0.22 kg m^{-2}) at WICA during the summer of 2012, which dominated over the
402 influence of the decadal maximum wildfire emissions (TFI = 0.021 g NO_x m^{-3}). An increasing
403 trend of 6.7 g m^{-2} yr^{-1} (p = 0.17) was found in total precipitation at WICA for the time period of
404 2005 – 2015, indicative of increasing cloudiness and ultimately contributing to the decreasing
405 trend in the A4DM8HA over the decade at this site.

406 Compared to YELL, CNTL, GTHC, ROMO, and WICA, sites located at the lower parts
407 of the basins (i.e., CANY, DINO, MEEK, RANG) had lower annual precipitation levels ranging
408 from 0.08 – 0.12 kg m^{-2} over 2005 – 2015 (Figure 9a). Significant negative correlations were
409 only found between summertime 5th percentile DM8HA O_3 and relative humidity at CANY,
410 MEEK, RANG (Table S6). This indicates a stronger impact of cloudiness associated with
411 precipitation weather on summertime baseline O_3 levels at sites within the basins.

412 **7. In situ photochemical O_3 production in winter and summer**

413 To determine the influence of in situ photochemical O_3 production on ambient O_3 in/near
414 O&NG basins, box model simulations were conducted for the Uintah-Piceance Basin, Denver-
415 Julesburg Basin, and its downwind region. In particular, field measurements of VOCs and NO_x
416 in the Uintah Basin during UBWOS 2012 – 2014 were used to understand the role of in situ

417 photochemistry in determining observed O_3 at RANG, DINO, and MEEK during winters of 2012
418 – 2014 (Figure 1). Measurements during FRAPPÉ at ROMO were used to determine
419 photochemically produced O_3 in summer 2014, while the NACHTT campaign at the Boulder
420 Atmospheric Observatory (BAO) Tower was used for winter 2011. Constraining the model
421 concentrations of VOCs, NO_x, and the radical precursors HCHO, HONO, and $ClNO_2$ using the
422 observed diel profiles reduced the impact of turbulent mixing and transport processes on the in
423 situ photochemical O_3 production. Figure 10 compares the observed average diel cycle of O_3
424 mixing ratios with those simulated for each campaign. Differences between observed and
425 simulated diel O_3 profiles represent the combined impact of transport processes, stratospheric
426 intrusion, and model uncertainty on surface O_3.

427 During NACHTT, photochemically produced O_3 at BAO ranged from 6 ppbv at 6:00 am
428 MST to 22 ppbv at 15:00 pm MST, contributing 20 – 52% of the observed O_3 (Figure 10a).
429 Photochemically produced O_3 contributed 30 – 60% of observed O_3 during UBWOS 2012
430 (Figure 10b). As seen in Figures 10c and 10d, it is possible for the contribution of
431 photochemically produced O_3 during UBWOS 2013 and UBWOS 2014 to exceed the
432 observations. For example, a modeled maximum value of 111 ppbv photochemically produced
433 O_3 was simulated for 16:00 pm MST during UBWOS 2013, larger than the 96 ppbv observed at
434 the site, which indicates that instantaneous mixing with surrounding air and fast transport
435 lowered the photochemically produced O_3 to the observed level.

436 The decadal highest winter seasonal median DM8HA O_3 was found at DINO (59 ppbv),
437 MEEK (44 ppbv), and RANG (44 ppbv) in winter 2013 (Figure 3c). A positive AO phase was
438 encountered during the winter of 2012 (Figure 5b), where the ambient conditions were relatively
439 warm without snow cover (Edwards et al., 2013), and the resulting conditions exhibited only

moderate O_3 production (~31 ppbv in Figure 10b). In contrast to 2012, winter 2013 was in a negative AO phase (Figure 6b), placing the Intermountain West under a strong influence of frigid Arctic air (Section 5) and subsequently under meteorologically stagnant conditions and increased snow cover within the basins. As a result, the high levels of VOC emissions from O&NG fields that accumulated in the shallow boundary layer coupled with the increased photolysis rates from the snow albedo contributed to rapid O_3 production (~78 ppbv in Figure 10c) within the basin, consistent with results from Edward et al. (2014). This result supports the point that surface O_3 at the sites within the basins was attributed mostly to in situ photochemical reactions (Section 5).

In contrast to the four wintertime campaigns described above, FRAPPÉ was conducted in the summer. The O_3 measurements from ROMO, located in the center of the FRAPPÉ campaign area, showed a diel cycle with ~40 ppbv nighttime and ~49 ppbv daytime O_3 levels. In contrast, photochemically produced O_3 at ROMO showed a distinct diel cycle with 0 ppbv at night and ~41 ppbv during the day. The strong diel cycle of photochemical production of O_3 at ROMO probably resulted from the combined effect of its high elevation and close proximity to the NFR. During the day, large amounts of O_3 precursors from the NFR transported upward from the southeast (Figure 5a) and contributed to photochemical O_3 production at ROMO (Benedict et al., 2018) followed by dramatically decreased photochemical production accompanied by the collapse of the planetary boundary layer during sunset at ~20:00 MST.

7.1 VOCs-NO_x-O_3 sensitivity

The O_3 sensitivity to NO_x and VOC emissions, which is relevant to the attainment of regional air quality standards, was evaluated in/near O&NG basins. Fifteen simulations for each field campaign were performed with scaled NO_x mixing ratios and the base case VOC scenario

to test the sensitivity of daily maximum photochemical O_3 production. The O_3 formation regime was found be associated to the AO. Photochemically produced O_3 during UBWOS 2012 and UBWOS 2014 was sensitive to VOCs (Figure 10f), indicating that O_3 photochemistry at DINO, RANG, and MEEK was also likely to be radical limited in winter 2012 and 2014. In contrast to these two winters, O_3 photochemistry had mixed sensitivity during UBWOS 2013 (Figure 10f), when in situ photochemically produced O_3 could be as high as 111 ppbv. Winter 2013 was in a negative AO phase, while winters of 2012 and 2014 were in positive phases. As stated in Section 5, surface O_3 at the sites within the basin was attributed mostly to in situ photochemical reactions. Therefore, for areas within the basins, emission reductions in VOCs alone would lead to O_3 mitigation in positive AO years, while emission reductions in both VOCs and NO_x would be effective in negative AO years. In the NFR region, photochemical O_3 production in winter 2011 surrounding BAO was sensitive to VOCs during NACHTT (Figure 10f). Photochemical O_3 production at ROMO in summer 2014 had mixed sensitivity (Figure 10f).

Edwards et al. (2013) also simulated an average UBWOS 2012 day (15 January to 1 March 2012) and found the same O_3 formation regime as our study. They found that the radical-limited O_3 photochemistry in 2012 was driven by the very low radical production rates (~2.3 ppbv day^{-1}) in comparison to the emission rate of NO_x. While an average UBWOS 2013 day (23 January to 24 March 2013) was simulated in our study, Edwards et al. (2014) simulated a single stagnant six-day (31 January to 5 February 2013) strong O_3 event, when DM8HA O_3 increased from 67 to 107 ppbv. It was found that O_3 in winter 2013 was sensitive to changes of NO_x, and the total net radical production rate could be as high as ~19 ppbv day^{-1}, which was sufficient to prevent NO_x saturation (Edward et al., 2014).

8. Summary

Our study suggested that decadal trends in the A4DM8HA over the Intermountain West during 2005 – 2015 were shaped by precipitation weather, wildfire emissions, stratospheric intrusion, and transport from the Arctic and the West Coast facilitated by regional to hemispheric circulation. Trends over the areas near/within O&NG basins were predominantly impacted by changes in emissions from the O&NG basins among other anthropogenic sources. Two reference sites, YELL and CRMO, exhibited no significant trends in the A4DM8HA O_3 over 2005 – 2015, indicating, without the immediate influence of O&NG emissions, relatively constant O_3 levels over the Intermountain West. In contrast, decadal trends in the A4DM8HA varied at the 11 sites located either in or near the O&NG extraction basins. A significant decreasing trend of -0.76 ppbv yr^{-1} at MEVE was associated with the decreasing natural gas production (37%) in the San Juan Basin, while a significant decreasing trend (-0.54 ppbv yr^{-1}) at CANY was predominately influenced by declining extraction of CBM in the Paradox Basin and emission reductions of 35% in electricity generation from coal. Increasing precipitation (6.7 g m^{-2} yr^{-1}) resulting from increasing cloudiness in the southern portion of the Black Hills contributed to the decreasing trend in the A4DM8HA (-1.21 ppbv yr^{-1}) at WICA. No trends were found in the 4DM8HA at the remaining sites, resulting likely from the combined effect of increasing emissions from O&NG extraction and decreasing emissions from other sectors.

In winter, seasonal 50^{th}/95^{th} DM8HA O_3 was associated with the AO at 8 sites, including the reference site YELL. For sites within the O&NG basins, O&NG emissions, colder surface air temperature, and enhanced solar radiation due to snow cover contributed to higher O_3, especially in the seasonal 95^{th} levels during negative AO years, and emission reductions in both VOCs and NO_x could lead to effective O_3 mitigation. For sites outside the O&NG basins, the high O_3 in seasonal 50^{th} levels were a result of transport from the Arctic or California and stratospheric

intrusion. In summer, the interannual variation of O_3 was predominantly affected by precipitation weather at 9 sites including the two reference sites. At high-elevation sites in the mountains, more abundant precipitation (0.18 – 0.27 kg m^{-2}) induced more cloudiness and consequently reduced solar flux leading less O_3 production in seasonal 5^{th}/50^{th}/95^{th} levels. However, at sites within the basin, the cloudiness associated with precipitation weather had a stronger impact on summertime baseline O_3 levels (i.e., the 5^{th} percentile).

This study is the first one to investigate the long term impact of O&NG extraction activities on the distribution and trend of surface O_3 over the intermountain U.S. O&NG activities have varied greatly over the past decade. In Wyoming, annual O&NG production levels have fallen significantly in the Jonah Field since 2009 and the Pinedale Field since 2012, because of lower natural gas prices relative to crude oil (http://wogcc.wyo.gov/). In Colorado, the number of active wells in Weld County increased by ~2000 between 2012 and 2014, followed by a decline since early 2015 (http://cogcc.state.co.us/data.html). However, current emission inventories underestimated VOC emissions from O&NG productions by a factor of 2 or more (Péron et al., 2014). While data analysis studies provided measurement-based estimates of contributions from various processes to decadal variability of surface O_3, we understand their limitation in clearly separating such contributions. Detailed multiyear studies that integrate measurements and three-dimensional chemical transport model simulations with accurate emission inventories are needed to further quantify the contribution of each process identified in this work.

Author Contributions

YZ and HM designed this study. BS provided long-term surface observations. YZ led the analysis and writing of this manuscript with significant contributions and comments from HM

and BS.

Acknowledgements

This work was supported by the Chemistry Emeriti Faulty Award from the Department of Chemistry at SUNY College of Environmental Science and Forestry and the National Park Service. We are grateful to Jessica Ward, Air Resources Specialists, Inc. for retrieving and providing the National Park Service data. We thank Cara Kesler for providing data from the Wyoming Department of Environmental Quality. We acknowledge the free use of tropospheric NO_2 column data from the OMI sensor from www.temis.nl. The assumptions, findings, conclusions, judgements, and views presented herein are those of the authors and should not be interpreted as necessarily representing the National Park Service.

References

Abeleira, A. J. and Farmer, D. K.: Summer ozone in the northern Front Range metropolitan area: weekend–weekday effects, temperature dependences, and the impact of drought. Atmos. Chem. Phys., 17, 6517-6529, https://doi.org/10.5194/acp-17-6517-2017, 2017.

Akagi, S. K., Yokelson, R. J., Wiedinmyer, C., Alvarado, M. J., Reid, J. S., Karl, T., Crounse, J. D., and Wennberg, P. O.: Emission factors for open and domestic biomass burning for use in atmospheric models. Atmos. Chem. Phys., 11, 4039-4072, https://doi.org/10.5194/acp-11-4039-2011, 2011.

Allen, D.T.: Atmospheric emissions and air quality impacts from natural gas production and use, Annu. Rev. Chem. Biomol. Eng. 5, 55-75, doi:10.1146/annurev-chembioeng-060713-035938, 2014.

Allen, D. T.: Emissions from oil and gas operations in the United States and their air quality implications, Journal of the Air & Waste Management Association, 66:6,549-575, DOI: 10.1080/10962247.2016.1171263, 2016.

Benedict, K. B., Zhou, Y., Sive, B. C., Prenni, A. J., Gebhart, K. A., Fischer, E. V., Evanoski-Cole, A., Sullivan, A. P., Callahan, S., Schichtel, B. A., Mao, H., Zhou, Y., and Collett Jr., J. L.: Volatile organic compounds and ozone in Rocky Mountain National Park during FRAPPÉ, Atmos. Chem. Phys., 19, 499-521, https://doi.org/10.5194/acp-19-499-2019, 2019.

Carter, W. P. L. and Seinfeld, J. H.: Winter ozone formation and VOC incremental reactivities in the Upper Green River Basin of Wyoming. Atmospheric Environment, 50, 255-266, https://doi.org/10.1016/j.atmosenv.2011.12.025, 2012

563 Chan, E.: Regional ground-level ozone trends in the context of meteorological influences across
564 Canada and the eastern United States from 1997 to 2006. Journal of Geophysical Research:
565 Atmospheres, 114, 1-18, https://doi.org/10.1029/2008JD010090, 2009.

566 Cooper, O. R., Gao, R. S., Tarasick, D., Leblanc, T., and Sweeney, C.: Long-term ozone trends
567 at rural ozone monitoring sites across the United States, 1990-2010. Journal of Geophysical
568 Research: Atmospheres, 117, 1990-2010, https://doi.org/10.1029/2012JD018261, 2012.

569 Draxler, R. R., and Hess, G. D.: NOAA Technical Memorandum ERL ARL-224, 28.
570 https://www.arl.noaa.gov/documents/reports/arl-224.pdf, 1998.

571 Edwards, P. M., Young, C. J., Aikin, K., deGouw, J., Dubé, W. P., Geiger, F., Gilman, J.,
572 Helmig, D., Holloway, J. S., Kercher, J., Lerner, B., Martin, R., McLaren, R., Parrish, D. D.,
573 Peischl, J., Roberts, J. M., Ryerson, T. B., Thornton, J., Warneke, C., Williams, E. J., and Brown,
574 S. S.: Ozone photochemistry in an oil and natural gas extraction region during winter:
575 simulations of a snow-free season in the Uintah Basin, Utah, Atmos. Chem. Phys., 13, 8955-
576 8971, https://doi.org/10.5194/acp-13-8955-2013, 2013.

577 Edwards, P.M., Brown, S.S., Roberts, J.M., Ahmadov, R., Banta, R.M., DeGouw, J. A., Dubé,
578 W.P., Field, R. A., Flynn, J.H., Gilman, J.B., Graus, M., Helmig, D., Koss, A., Langford, A.O.,
579 Lefer, B.L., Lerner, B.M., Li, R., Li, S.-M., McKeen, S. A., Murphy, S.M., Parrish, D.D., Senff,
580 C.J., Soltis, J., Stutz, J., Sweeney, C., Thompson, C.R., Trainer, M.K., Tsai, C., Veres, P.R.,
581 Washenfelder, R. a., Warneke, C., Wild, R.J., Young, C.J., Yuan, B., Zamora, R: High winter
582 ozone pollution from carbonyl photolysis in an oil and gas basin. Nature, 514(7522), 351-354,
583 https://doi.org/10.1038/nature13767, 2014.

584 Energy Information Administration (EIA): Shale in the United States. Retrieved from
585 http://www.eia.gov/energy_in_brief/article/shale_in_the_united_states.cfm, 2015.

586 Environmental Protection Agency (EPA): Regulatory Actions | Ground-level Ozone | US EPA.
587 Retrieved February 8, 2016, from http://www3.epa.gov/ozonepollution/actions.html, 2015.

588 Helmig, D., Thompson, C. R., Evans, J., Boylan, P., Hueber, J., and Park, J.-H.: Highly elevated
589 atmospheric levels of volatile organic compounds in the Uintah Basin, Utah. Environmental
590 Science & Technology, 48, 4707-4715, https://doi.org/10.1021/es405046r, 2014.

591 Gaudel, A., Cooper, O.R., Ancellet, G., Barret, B., Boynard, A., Burrows, J.P., Clerbaux, C.,
592 Coheur, P.-F., Cuesta, J., Cuevas, E., Doniki, S., Dufour, G., Ebojie, F., Foret, G., Garcia, O.,
593 Granados Muños, M.J., Hannigan, J.W., Hase, F., Huang, G., Hassler, B., Hurtmans, D., Jaffe,
594 D., Jones, N., Kalabokas, P., Kerridge, B., Kulawik, S.S., Latter, B., Leblanc, T., Le Flochmoën,
595 E., Lin, W., Liu, J., Liu, X., Mahieu, E., McClure-Begley, A., Neu, J.L., Osman, M., Palm, M.,
596 Petetin, H., Petropavlovskikh, I., Querel, R., Rahpoe, N., Rozanov, A., Schultz, M.G., Schwab, J.,
597 Siddans, R., Smale, D., Steinbacher, M., Tanimoto, H., Tarasick, D.W., Thouret, V., Thompson,
598 A.M., Trickl, T., Weatherhead, E., Wespes, C., Worden, H.M., Vigouroux, C., Xu, X., Zeng, G.
599 and Ziemke, J.: Tropospheric Ozone Assessment Report: Present-day distribution and trends of
600 tropospheric ozone relevant to climate and global atmospheric chemistry model evaluation. Elem
601 Sci Anth, 6, p.39, http://doi.org/10.1525/elementa.291, 2018.

602 Hess, P. G. and Lamarque, J. F.: Ozone source attribution and its modulation by the Arctic
603 oscillation during the spring months. Journal of Geophysical Research: Atmospheres, 112, 1-17,
604 https://doi.org/10.1029/2006JD007557, 2007.

605 Huang, M., Bowman, K. W., Carmichael, G. R., Bradley, P. R., Worden, H. M., Luo, M., Cooper,
606 O. R., Pollack, I. B., Ryerson, T. B., Brown, S. S.: Impact of Southern California anthropogenic
607 emissions on ozone pollution in the mountain states: Model analysis and observational evidence
608 from space. Journal of Geophysical Research: Atmospheres, 118, 12,784-12,803,
609 https://doi.org/10.1002/2013JD020205, 2013.

610 Jaffe, D., Chand, D., Hafner, W., Westerling, A., and Spracklen, D.: Influence of Fires on O3
611 Concentrations in the Western U.S. Environmental Science & Technology, 42, 5885-5891,
612 https://doi.org/10.1021/es800084k, 2008.

613 Jaffe, D. A. and Wigder, N. L.: Ozone production from wildfires: A critical review. Atmospheric
614 Environment, 51, 1-10, https://doi.org/10.1016/j.atmosenv.2011.11.063, 2012.

615 Jenkin, M. E., Young, J. C., and Rickard, A. R.: The MCM v3.3.1 degradation scheme for
616 isoprene. Atmos. Chem. Phys., 15, 11433-11459, https://doi.org/10.5194/acp-15-11433-2015,
617 2015.

618 Karion, A., Sweeney, C., Petron, G., Frost, G., Hardesty, R. M., Kofler, J., Miller, B. R.,
619 Newberger, T., Wolter, S., Banta, R., Brewer, A., Dlugokencky, E., Lang, P., Montzka, S. A.,
620 Schnell, R., Tans, P., Trainer, M., Zamora, R., Conley, S.: Methane emissions estimate from
621 airborne measurements over a western United States natural gas field Geophys. Res. Lett., 40,
622 4393-4397, DOI: 10.1002/grl.50811, 2013.

623 Knote, C., Tuccella, P., Curci, G., Emmons, L., Orlando, J.J., Madronich, S., Baró, R., Jiménez-
624 Guerrero, P., Luecken, D., Hogrefe, C., Forkel, R., Werhahn, J., Hirtl, M., Pérez, J.L., San José,
625 R., Giordano, L., Brunner, D., Yahya, K., Zhang, Y.: Influence of the choice of gas-phase
626 mechanism on predictions of key gaseous pollutants during the AQMEII phase-2
627 intercomparison. Atmospheric Environment, 115, 553-568, https://doi.org/10.1016/j.atmosen
628 v.2014.11.066, 2015.

629 Lin, M., Horowitz, L. W., Payton, R., Fiore, A. M., and Tonnesen, G.: US surface ozone trends
630 and extremes from 1980 to 2014: quantifying the roles of rising Asian emissions, domestic
631 controls, wildfires, and climate. Atmos. Chem. Phys., 17, 2943-2970, https://doi.org/10.51
632 94/acp-17-2943-2017, 2017.

633 Lin, M., Horowitz, L. W., Oltmans, S. J., Fiore, A. M., and Fan, S.: Tropospheric ozone trends at
634 Mauna Loa Observatory tied to decadal climate variability. Nature Geoscience, 7, 136-143,
635 https://doi.org/10.1038/ngeo2066, 2014.

636 Lu, X., Zhang, L., Yue, X., Zhang, J., Jaffe, D. A., Stohl, A., Zhao, Y., and Shao, J.: Wildfire
637 influences on the variability and trend of summer surface ozone in the mountainous western
638 United States, Atmos. Chem. Phys., 16, 14687-14702, https://doi.org/10.5194/acp-16-14687-
639 2016, 2016.

Madronich, S., McKenzie, R. L., Björn, L. O., and Caldwell, M. M.: Changes in biologically active ultraviolet radiation reaching the Earth's surface. Journal of Photochemistry and Photobiology B: Biology, 46, 5-19, https://doi.org/10.1016/S1011-1344(98)00182-1, 1998.

Natural Gas Intelligence (NGI): Major & Minor Resource Plays. Retrieved April 27, 2018, from http://www.naturalgasintel.com/Major-and-Minor-North-American-Shale-Basins-and-Resource-Plays, 2018.

McDuffie, E. E., Edwards, P. M., Gilman, J. B., Lerner, B. M., Dubé, W. P., Trainer, M., Wolfe, D. E., Angevine, W. M., deGouw, J., Williams, E. J., Tevlin, A. G., Murphy, J. G., Fischer, E. V., McKeen, S., Ryerson, T. B., Peischl, J., Holloway, J. S., Aikin, K., Langford, A. O., Senff, C. J., Alvarez, R. J., Hall, S. R., Ullmann, K., Lantz, K. O., Brown, S. S.: Influence of oil and gas emissions on summertime ozone in the Colorado Northern Front Range. Journal of Geophysical Research: Atmospheres, 121, 8712-8729, https://doi.org/10.1002/2016JD025265, 2016.

Monks, P.S., Granier, C., Fuzzi, S., Stohl, A., Williams, M.L., Akimoto, H., Amann, M., Baklanov, A., Baltensperger, U., Bey, I., Blake, N., Blake, R.S., Carslaw, K., Cooper, O.R., Dentener, F., Fowler, D., Fragkou, E., Frost, G.J., Generoso, S., Ginoux, P., Grewe, V., Guenther, A., Hansson, H.C., Henne, S., Hjorth, J., Hofzumahaus, A., Huntrieser, H., Isaksen, I.S.A., Jenkin, M.E., Kaiser, J., Kanakidou, M., Klimont, Z., Kulmala, M., Laj, P., Lawrence, M.G., Lee, J.D., Liousse, C., Maione, M., McFiggans, G., Metzger, A., Mieville, A., Moussiopoulos, N., Orlando, J.J., O'Dowd, C.D., Palmer, P.I., Parrish, D.D., Petzold, A., Platt, U., Pöschl, U., Prévôt, A.S.H., Reeves, C.E., Reimann, S., Rudich, Y., Sellegri, K., Steinbrecher, R., Simpson, D., ten Brink, H., Theloke, J., van der Werf, G.R., Vautard, R., Vestreng, V., Vlachokostas, C., von Glasow, R.: Atmospheric composition change – global and regional air quality. Atmospheric Environment, 43, 5268-5350, https://doi.org/10.1016/j.atmosenv.2009.08.021, 2009.

Parrish, D.D., Law, K.S., Staehelin, J., Derwent, R., Cooper, O.R., Tanimoto, H., Volz-Thomas, A., Gilge, S., Scheel, H.E., Steinbacher, M., Chan, E.: Long-term changes in lower tropospheric baseline ozone concentrations at northern mid-latitudes. Atmos. Chem. Phys., 12, 11485-11504, https://doi.org/10.5194/acp-12-11485-2012, 2012.

Parrish, D.D., Law, K.S., Staehelin, J., Derwent, R., Cooper, O.R., Tanimoto, H., Volz-Thomas, A., Gilge, S., Scheel, H.E., Steinbacher, M., Chan, E.: Lower tropospheric ozone at northern midlatitudes: Changing seasonal cycle. Geophysical Research Letters, 40, 1631-1636, https://doi.org/10.1002/grl.50303, 2013.

Pétron, G., Karion, A., Sweeney, C., Miller, B.R., Montzka, S.A., Frost, G.J., Trainer, M., Tans, P., Andrews, A., Kofler, J., Helmig, D., Guenther, D., Dlugokencky, E., Lang, P., Newberger, T., Wolter, S., Hall, B., Novelli, P., Brewer, A., Conley, S., Hardesty, M., Banta, R., White, A., Noone, D., Wolfe, D., Schnell, R.: A new look at methane and nonmethane hydrocarbon emissions from oil and natural gas operations in the Colorado Denver-Julesburg Basin. Journal of Geophysical Research: Atmospheres, 119, 6836-6852, https://doi.org/10.1002/2013JD021272, 2014.

Pfister G. G., Reddy P. J., Barth M. C., Flocke F. F., Fried A., Herndon S. C., Sive B. C., Sullivan J. T., Thompson A. M., Yacovitch T. I., Weinheimer A. J., Wisthaler A.: Using

Observations and Source-Specific Model Tracers to Characterize Pollutant Transport During FRAPPÉ and DISCOVER-AQ. Journal of Geophysical Research: Atmospheres, 122, 10,510-10,538, https://doi.org/10.1002/2017JD027257, 2007.

Rappenglück, B., Ackermann, L., Alvarez, S., Golovko, J., Buhr, M., Field, R. A., Soltis, J., Montague, D. C., Hauze, B., Adamson, S., Risch, D., Wilkerson, G., Bush, D., Stoeckenius, T., and Keslar, C.: Strong wintertime ozone events in the Upper Green River basin, Wyoming, Atmos. Chem. Phys., 14, 4909-4934, https://doi.org/10.5194/acp-14-4909-2014, 2014.

Reddy, P. J. and Pfister, G. G.: Meteorological factors contributing to the interannual variability of midsummer surface ozone in Colorado, Utah, and other western U.S. states. Journal of Geophysical Research: Atmospheres, 121, 2434-2456, https://doi.org/10.1002/2015JD023840, 2016.

Reidmiller, D. R., Fiore, A. M., Jaffe, D. A., Bergmann, D., Cuvelier, C., Dentener, F. J., Duncan, B. N., Folberth, G., Gauss, M., Gong, S., Hess, P., Jonson, J. E., Keating, T., Lupu, A., Marmer, E., Park, R., Schultz, M. G., Shindell, D. T., Szopa, S., Vivanco, M. G., Wild, O., and Zuber, A.: The influence of foreign vs. North American emissions on surface ozone in the US, Atmos. Chem. Phys., 9, 5027-5042, https://doi.org/10.5194/acp-9-5027-2009, 2009.

Rodriguez, M. A., Barna, M. G., and Moore, T.: Regional Impacts of Oil and Gas Development on Ozone Formation in the Western United States. Journal of the Air & Waste Management Association, 59, 1111-1118, https://doi.org/10.3155/1047-3289.59.9.1111, 2009.

Ryerson T. B., Andrews A. E., Angevine W. M., Bates T. S., Brock C. A., Cairns B., Cohen R. C., Cooper O. R., Gouw J. A., Fehsenfeld F. C., Ferrare R. A., Fischer M. L., Flagan R. C., Goldstein A. H., Hair J. W., Hardesty R. M., Hostetler C. A., Jimenez J. L., Langford A. O., McCauley E., McKeen S. A., Molina L. T., Nenes A., Oltmans S. J., Parrish D. D., Pederson J. R., Pierce R. B., Prather K., Quinn P. K., Seinfeld J. H., Senff C. J., Sorooshian A., Stutz J., Surratt J. D., Trainer M., Volkamer R., Williams E. J., Wofsy S. C.: The 2010 California Research at the Nexus of Air Quality and Climate Change (CalNex) field study. Journal of Geophysical Research: Atmospheres, 118, 5830-5866, https://doi.org/10.1002/jgrd.50331, 2013.

Schnell, R. C., Oltmans, S. J., Neely, R. R., Endres, M. S., Molenar, J. V., and White, A. B.: Rapid photochemical production of ozone at high concentrations in a rural site during winter. Nature Geoscience, 2, 120-122, https://doi.org/10.1038/ngeo415, 2009.

Stohl A., Bonasoni P., Cristofanelli P., Collins W., Feichter J., Frank A., Forster C., Gerasopoulos E., Gäggeler H., James P., Kentarchos T., Kromp-Kolb H., Krüger B., Land C., Meloen J., Papayannis A., Priller A., Seibert P., Sprenger M., Roelofs G. J., Scheel H. E., Schnabel C., Siegmund P., Tobler L., Trickl T., Wernli H., Wirth V., Zanis P., Zerefos C.: Stratosphere-troposphere exchange: A review, and what we have learned from STACCATO. Journal of Geophysical Research: Atmospheres, 108, https://doi.org/10.1029/2002JD002490, 2003.

Swarthout, R. F., Russo, R. S., Zhou, Y., Hart, A. H., and Sive, B. C.: Volatile organic compound distributions during the NACHTT campaign at the Boulder Atmospheric Observatory:

719 Influence of urban and natural gas sources. Journal of Geophysical Research: Atmospheres, 118,
720 10,614-10,637, https://doi.org/10.1002/jgrd.50722, 2013.

721 Thompson, T. M., D. Shepherd, A. Stacy, M. G. Barna, and B. A. Schichtel: Modeling to
722 Evaluate Contribution of Oil and Gas Emissions to Air Pollution, Journal of the Air & Waste
723 Management Association, 67, 445-461, DOI:10.1080/10962247.2016.1251508, 2017.

724 Westerling, A. L., Hidalgo, H. G., Cayan, D. R., and Swetnam, T. W.: Warming and Earlier
725 Spring Increase Western U.S. Forest Wildfire Activity. Science, 313, 940-943,
726 https://doi.org/10.1126/science.1128834, 2006.

727 Williams, P. and Peck, E. L.: Terrain Influences on Precipitation in the Intermountain West as
728 Related to Synoptic Situations. Journal of Applied Meteorology, 1, 343-347,
729 https://doi.org/10.1175/1520-0450(1962)001<0343:TIOPIT>2.0.CO;2, 1962.

730 Zhou, Y., Mao, H., Demerjian, K., Hogrefe, C., and Liu, J.: Regional and hemispheric influences
731 on temporal variability in baseline carbon monoxide and ozone over the Northeast US.
732 Atmospheric Environment, 164, 309-324, https://doi.org/10.1016/j.atmosenv.2017.06.017, 2017.

733

734

735

736

737

738

739

740

741

742

743

744

745

746

747

Atmos. Chem. Phys. Discuss., https://doi.org/10.5194/acp-2019-164
Manuscript under review for journal Atmos. Chem. Phys.
Discussion started: 19 March 2019

Atmospheric Chemistry and Physics Discussions

748 Table 1. Correlation coefficients (r) and p-value in parenthesis between the pairs of variables in winter over 2006 –
749 2015. Partial correlation was computed for surface temperature and seasonal 95th DM8HA by controlling the effect
750 of PV. Boldfaced numbers indicate p-value ≤ 0.10.

		r (O_3 vs AO)				r (O_3 vs Temperature)			Partial r
Site	Time Period	5th	50th	95th	r (AO vs temperature)	5th	50th	95th	95th
CANY	2006 - 2015	**-0.63 (0.05)**	**-0.72 (0.02)**	**-0.73 (0.02)**	**0.66 (0.04)**	**-0.81 (<0.01)**	**-0.64 (0.05)**	**-0.64 (0.04)**	**-0.62 (0.06)**
CAMP	2006 - 2015	0.06 (0.88)	-0.15 (0.67)	-0.30 (0.40)	0.31 (0.38)	0.11 (0.75)	-0.36 (0.31)	-0.21 (0.55)	-0.27 (0.49)
DINO	2011 - 2015	-0.29 (0.64)	**-0.89 (0.04)**	**-0.94 (0.02)**	**0.90 (0.04)**	-0.53 (0.36)	**-0.94 (0.02)**	**-0.96 (0.01)**	**-0.95 (0.05)**
MEEK	2011 - 2015	**-0.88 (0.02)**	**-0.91 (0.01)**	**-0.92 (0.01)**	**0.93 (0.02)**	**-0.84 (0.07)**	**-0.91 (0.03)**	**-0.85 (0.06)**	**-0.96 (0.04)**
RANG	2011 - 2015	-0.05 (0.93)	**-0.91 (0.03)**	**-0.93 (0.02)**	**0.92 (0.03)**	-0.38 (0.53)	**-0.99 (<0.01)**	**-0.95 (0.01)**	**-0.92 (0.08)**
MEVE	2006 - 2015	-0.53 (0.11)	**-0.70 (0.02)**	**-0.64 (0.04)**	0.53 (0.12)	**-0.54 (0.10)**	**-0.63 (0.05)**	**-0.59 (0.07)**	-0.28 (0.47)
ROMO	2006 - 2015	-0.09 (0.81)	**-0.72 (0.01)**	-0.49 (0.15)	0.50 (0.14)	-0.36 (0.31)	-0.48 (0.16)	-0.21 (0.56)	-0.14 (0.72)
WICA	2006 - 2014	0.25 (0.52)	**-0.58 (0.10)**	-0.39 (0.21)	0.26 (0.46)	-0.28 (0.51)	-0.50 (0.21)	-0.50 (0.20)	-0.49 (0.26)
CNTL	2006 - 2015	-0.04 (0.91)	-0.47 (0.17)	-0.38 (0.28)	-0.32 (0.37)	**0.63 (0.05)**	**0.73 (0.02)**	**0.66 (0.04)**	**0.66 (0.05)**
GTHC	2006 - 2015	-0.15 (0.67)	-0.03 (0.93)	0.04 (0.92)	**0.58 (0.08)**	-0.35 (0.32)	-0.23 (0.52)	-0.44 (0.20)	-0.55 (0.12)
PNDE	2006 - 2015	-0.29 (0.42)	-0.46 (0.18)	-0.05 (0.89)	0.30 (0.40)	-0.27 (0.45)	-0.09 (0.80)	-0.43 (0.21)	**-0.63 (0.07)**
CRMO	2008 - 2015	-0.41 (0.31)	-0.28 (0.51)	-0.10 (0.82)	0.53 (0.11)	-0.54 (0.16)	**-0.72 (0.04)**	-0.55 (0.16)	**-0.85 (0.01)**
YELL	2006 - 2015	**-0.68 (0.03)**	**-0.77 (<0.01)**	-0.46 (0.19)	0.37 (0.15)	**-0.63 (0.05)**	-0.43 (0.22)	-0.43 (0.22)	-0.37 (0.32)

751
752
753
754
755
756
757
758
759
760
761
762
763

Atmos. Chem. Phys. Discuss., https://doi.org/10.5194/acp-2019-164
Manuscript under review for journal Atmos. Chem. Phys.
Discussion started: 19 March 2019

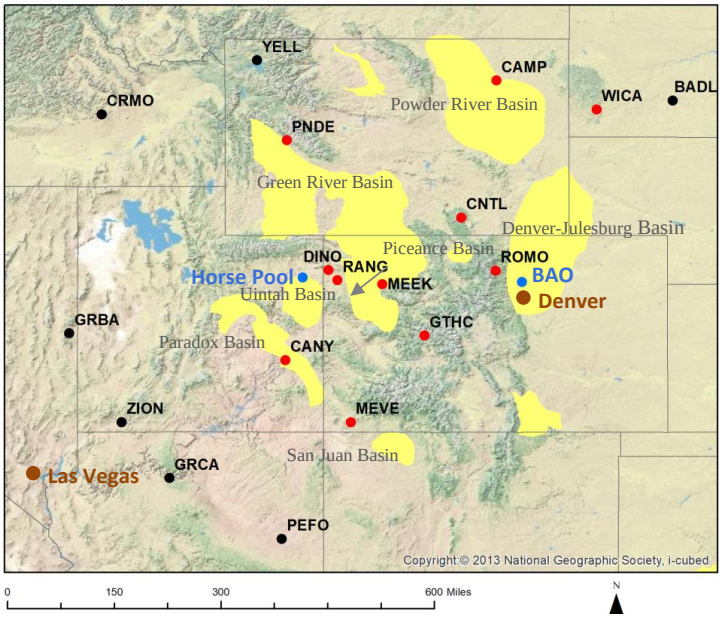

Figure 1. Topographic map of the mountain states with tight O&NG plays in the basins highlighted in yellow (https://www.eia.gov/). Eleven sites are located within 100km of a shale play (red dots), while seven sites are located at the periphery of the shale play (black dots). Blue dots show two campaign locations, Horse Pool and Boulder Atmospheric Observatory (BAO).

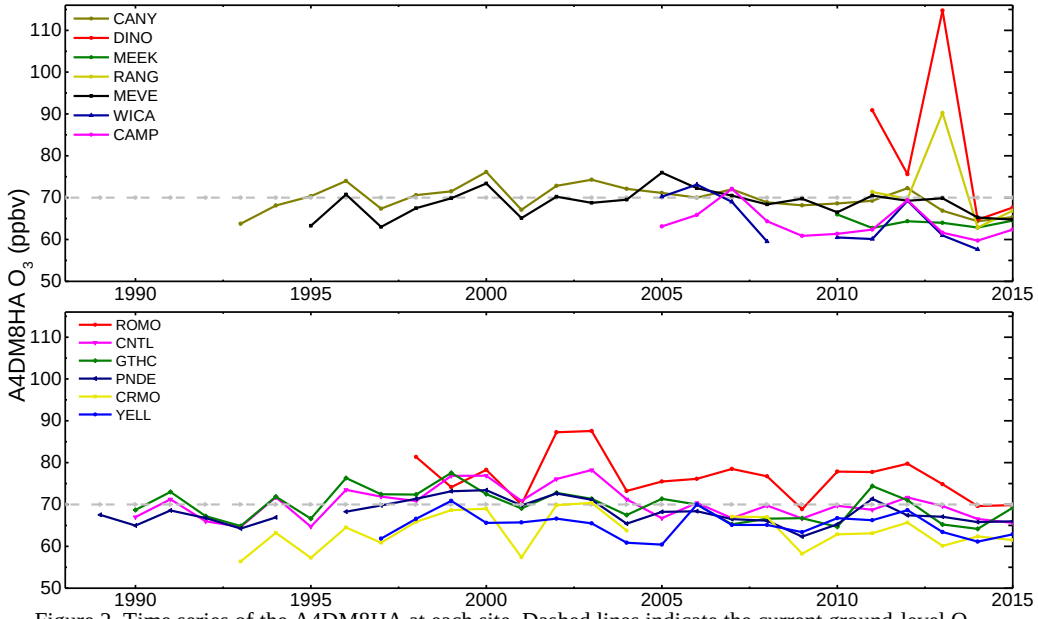

Figure 2. Time series of the A4DM8HA at each site. Dashed lines indicate the current ground-level O_3 standard (70 ppbv).

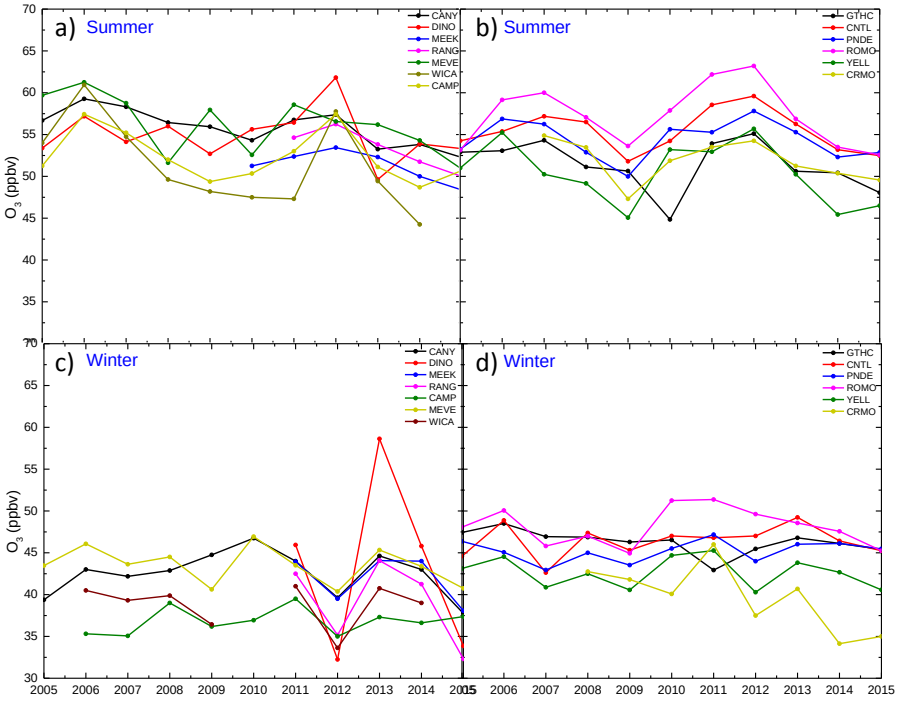

Figure 3. Time series of seasonal median values of DM8HA O_3 at each site in summer (a-b) and winter (c-d).

Atmos. Chem. Phys. Discuss., https://doi.org/10.5194/acp-2019-164
Manuscript under review for journal Atmos. Chem. Phys.
Discussion started: 19 March 2019

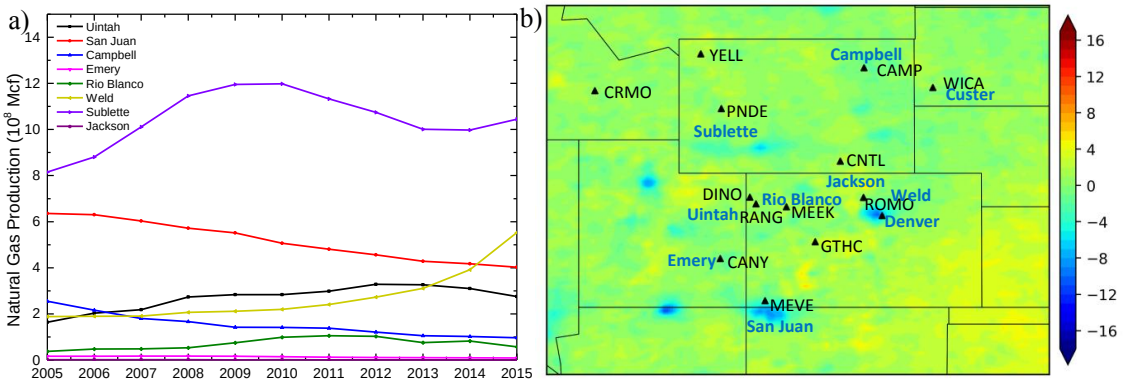

Figure 4. (a) Annual natural gas production in the counties that located in the O&NG basins over 2005 – 2015 (Data sources: the Utah Oil and Gas Program, https://oilgas.ogm.utah.gov/oilgasweb/index.xhtml; the Colorado Oil&Gas Conservation Commission, http://cogcc.state.co.us/data.html; the Wyoming Oil&Gas Conservation Commission, http://wogcc.wyo.gov/; the New Mexico Oil Conservation Division, http://www.emnrd.state.nm.us/ocd/). (b) The difference of OMI tropospheric NO_2 column densities (10^{14} molec.cm^{-2}) in summer between periods of 2005 – 2010 and 2011 – 2015 (Data source: Tropospheric Emission Monitoring Internet Service (TEMIS), www.temis.nl).

Atmos. Chem. Phys. Discuss., https://doi.org/10.5194/acp-2019-164
Manuscript under review for journal Atmos. Chem. Phys.
Discussion started: 19 March 2019

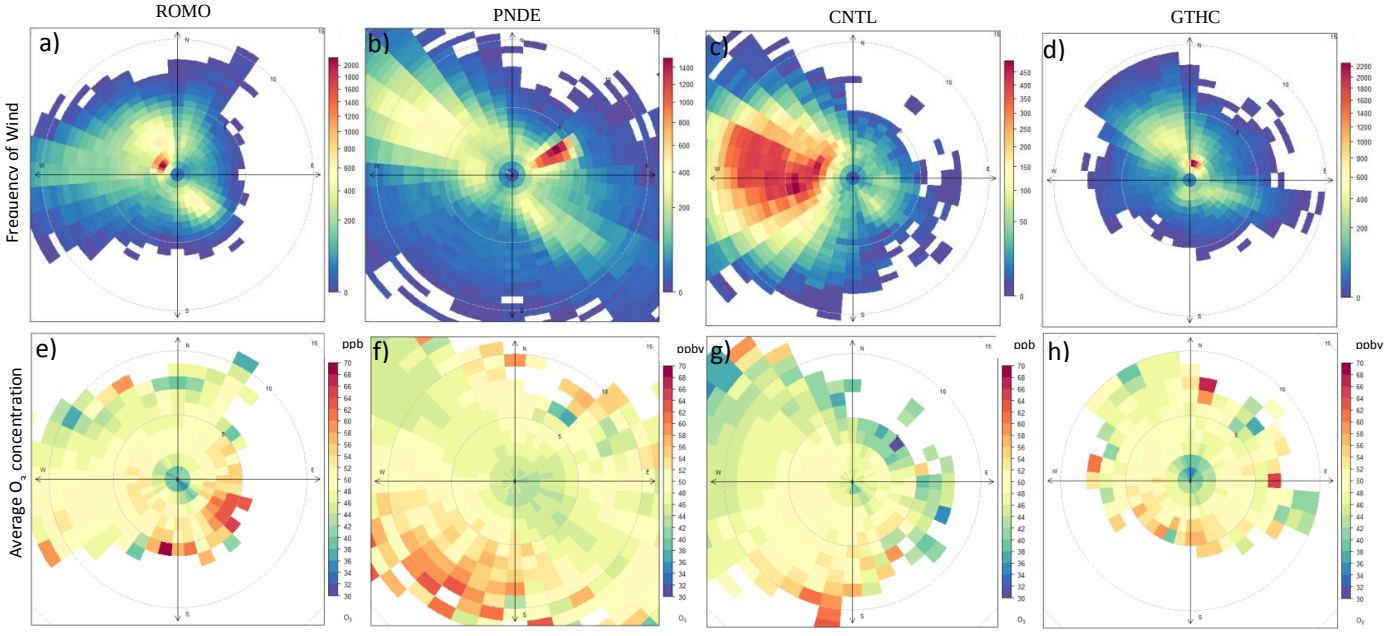

Figure 5. Frequency of wind (a-d) and average O_3 concentrations (ppbv) (e-h) binned by wind speed and wind direction at ROMO (a, e), PNDE (b, f), CNTL (c, g), and GTHC (d, h) over 2005 – 2015.

826

827

828

829

830

831

832

833

834

835

836

Atmos. Chem. Phys. Discuss., https://doi.org/10.5194/acp-2019-164
Manuscript under review for journal Atmos. Chem. Phys.
Discussion started: 19 March 2019

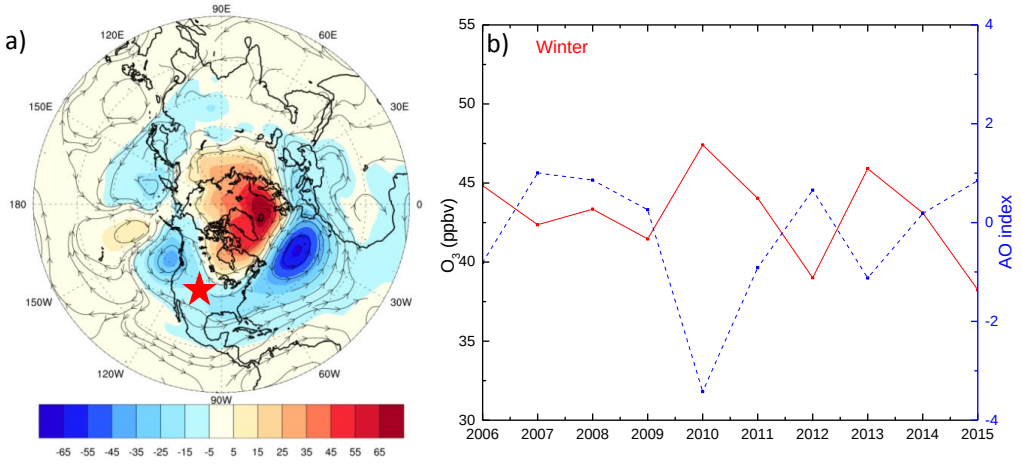

Figure 6. (a) The difference of geopotential height (m) and streamlines at 850 hPa between the high (2006, 2008, 2010, 2011, 2013) and low O_3 years (2007, 2009, 2012, 2014, 2015). (b) Time series of median DM8HA O_3 averaged over the study region and the AO index in winter. The red star indicates the study region. (Source: NCEP/NCAR reanalysis)

Atmos. Chem. Phys. Discuss., https://doi.org/10.5194/acp-2019-164
Manuscript under review for journal Atmos. Chem. Phys.
Discussion started: 19 March 2019

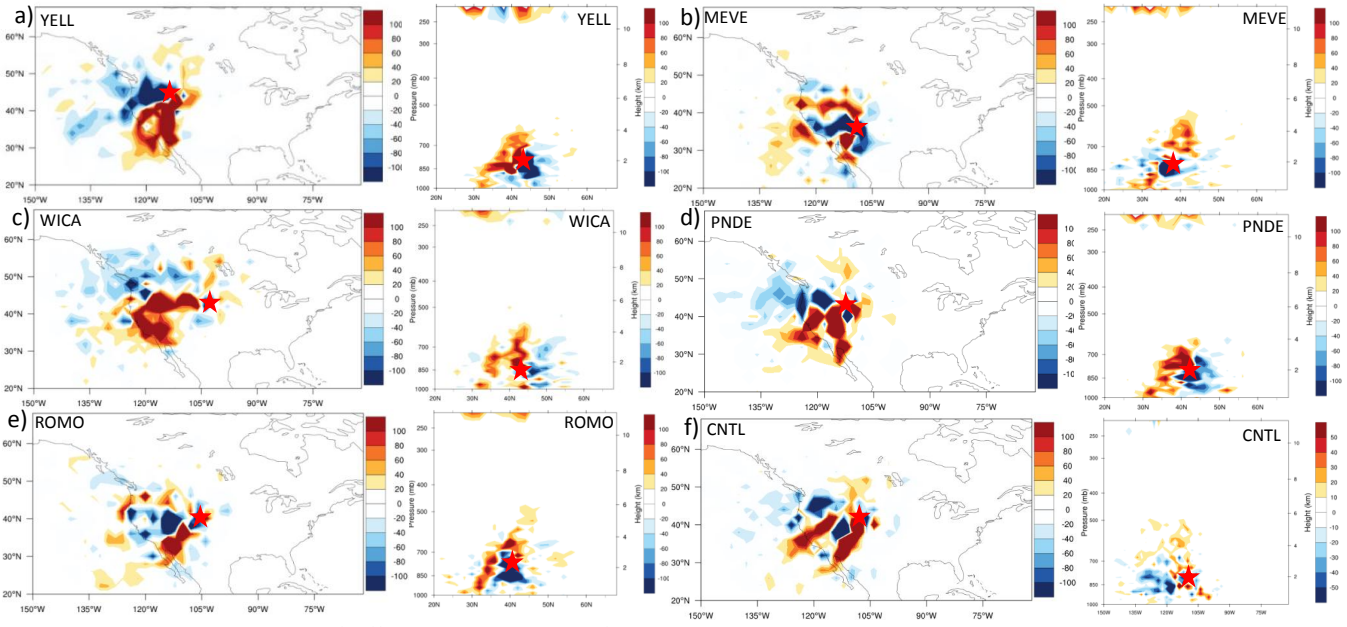

Figure 7. Maps and cross sections of differences in the number of 5-day backward trajectories originating at (a) YELL, (b) MEVE, (c) WICA, (d) PNDE, (e) ROMO, and (f) CNTL between high (2006, 2008, 2010, 2011, 2013) and low O_3 years (2007, 2009, 2012, 2014, 2015). Red stars indicate study sites.

Atmos. Chem. Phys. Discuss., https://doi.org/10.5194/acp-2019-164
Manuscript under review for journal Atmos. Chem. Phys.
Discussion started: 19 March 2019

Atmospheric Chemistry and Physics Discussions

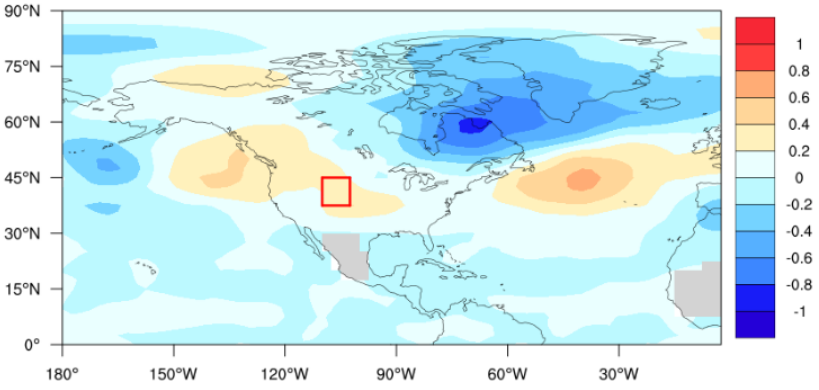

Figure 8. The difference of PV (10^{-6} $m^2 s^{-1} kg^{-1} K$) at 315 K between the high O_3 years (2006, 2008, 2010, 2011, 2013) and low O_3 years (2007, 2009, 2012, 2014, 2015). (Source: NCEP/NCAR reanalysis)

Atmos. Chem. Phys. Discuss., https://doi.org/10.5194/acp-2019-164
Manuscript under review for journal Atmos. Chem. Phys.
Discussion started: 19 March 2019

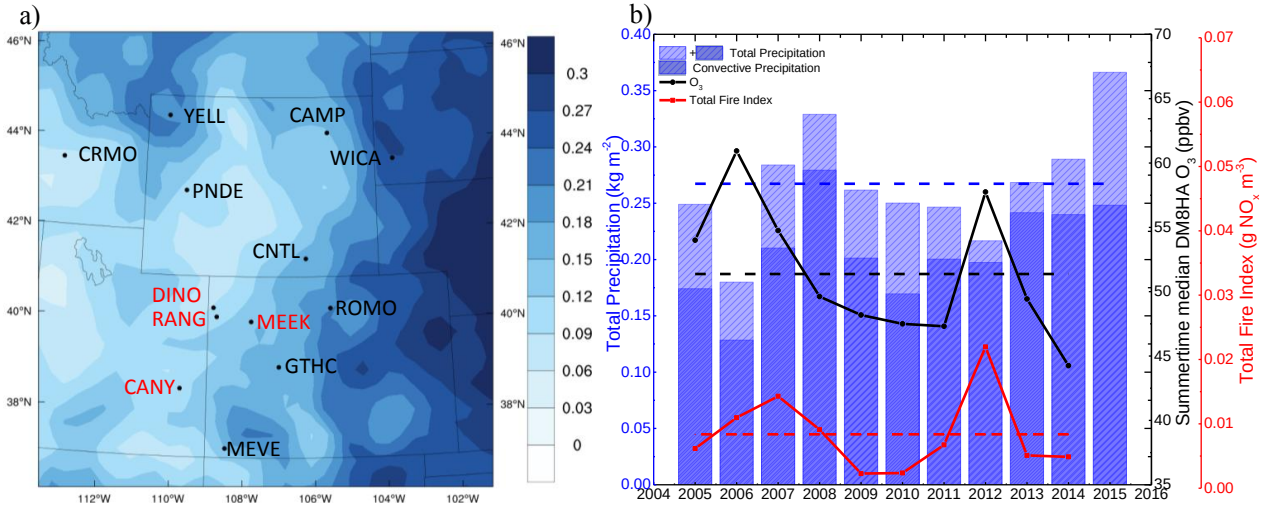

Figure 9. (a) Decadal average summertime total precipitation (kg m^{-2}) over 2005 – 2015, and the sites with low precipitation levels highlighted in red. (b) Time series of summer seasonal median DM8HA O_3, convective precipitation, total precipitation, and total fire index at WICA.

Atmos. Chem. Phys. Discuss., https://doi.org/10.5194/acp-2019-164
Manuscript under review for journal Atmos. Chem. Phys.
Discussion started: 19 March 2019

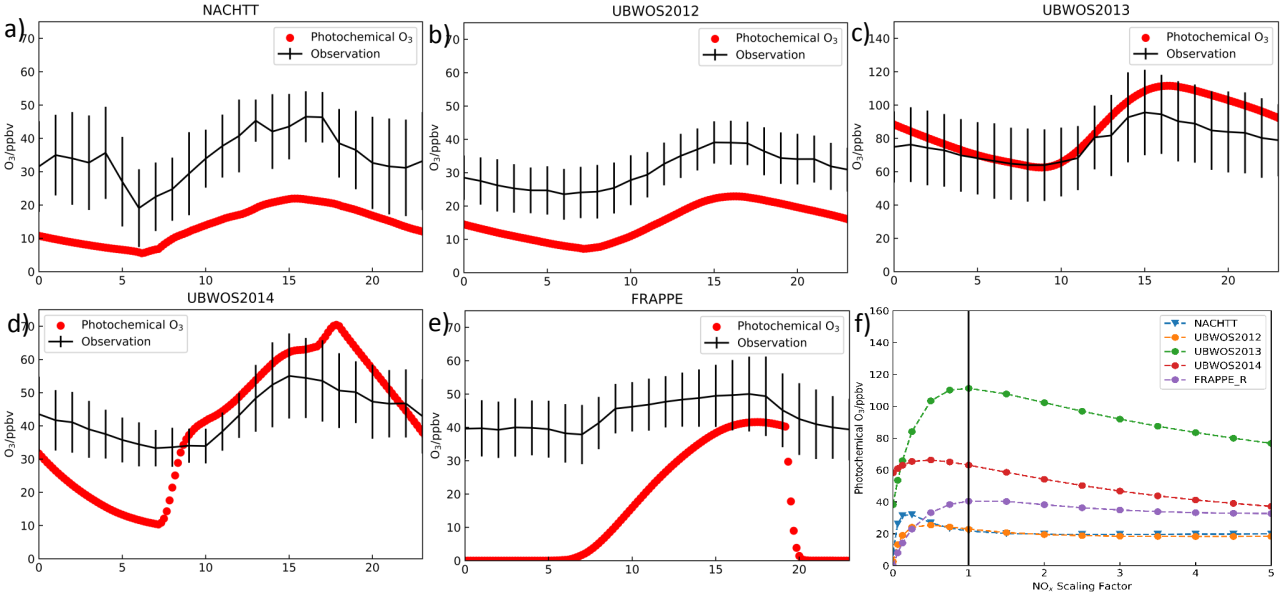

Figure 10. (a)-(e) Observed diel O_3 profile (black) and fully constrained base model calculated (red) for five campaigns. (f) NO_x sensitivity of maximum photochemical O_3 during each campaign.

889

890

891